Infrared Absorption Study of the Heme Pocket Dynamics of Carbonmonoxyheme Proteins

Andras D. Kaposi,* Jane M. Vanderkooi,† and Solomon S. Stavrov‡

*Department of Biophysics and Radiation Biology, Semmelweis University, Budapest, Hungary; †Johnson Research Foundation, Department of Biochemistry and Biophysics, University of Pennsylvania School of Medicine, Philadelphia, Pennsylvania; and ‡Sackler Institute of Molecular Medicine, Department of Human Genetics and Molecular Medicine, Sackler School of Medicine, Tel Aviv University, Tel Aviv, Israel

ABSTRACT The temperature dependencies of the infrared absorption CO bands of carboxy complexes of horseradish peroxidase (HRP(CO)) in glycerol/water mixture at pH 6.0 and 9.3 are interpreted using the theory of optical absorption bandshape. The bands' anharmonic behavior is explained assuming that there is a higher-energy set of conformational substates (CSS_h), which are populated upon heating and correspond to the protein substates with disordered water molecules in the heme pocket. Analysis of the second moments of the CO bands of the carboxy complexes of myoglobin (Mb(CO)) and hemoglobin (Hb(CO)), and of HRP(CO) with benzohydroxamic acid (HRP(CO)+BHA), shows that the low energy CSS_h exists also in the open conformation of Mb(CO), where the heme pocket is spacious enough to accommodate a water molecule. In the HRP(CO)+BHA and closed conformations of Mb(CO) and Hb(CO), the heme pocket is packed with BHA and different amino acids, the CSS_h has much higher energy and is hardly populated even at the highest temperatures. Therefore only motions of these amino acids contribute to the band broadening. These motions are linked to the protein surface and frozen in the glassy matrix, whereas in the liquid solvent they are harmonic. Thus the second moment of the CO band is temperature-independent in glass and is proportional to the temperature in liquid. The temperature dependence of the second moment of the CO peak of HRP(CO) in the trehalose glass exhibits linear coupling to an oscillator. This oscillator can be a moving water molecule locked in the heme pocket in the whole interval of temperatures or a trehalose molecule located in the heme pocket.

INTRODUCTION

Heme proteins (e.g., myoglobin, Mb, and hemoglobin, Hb) significantly change configuration upon coordination of different ligands and can be studied using virtually all spectroscopic techniques covering wide intervals of times and temperatures. Therefore they are intensively used to address the problem of protein dynamics and its role in the protein functioning (1,2). The role of protein dynamics in influencing the protein function was shown by studies of CO recombination in myoglobin (Mb) after photolysis. These studies have led to the view of conformational substates (CSS) and energy barriers between them (3,4). The authors explained nonexponential kinetics of the ligand rebinding at low temperatures, postulating that, in the glassy matrix, the protein molecules are frozen in slightly different conformations, corresponding to various CSSs. Existence of CSSs was supported by the observation that proteins containing heme derivatives show inhomogeneously broadened optical spectra (5–8). Consequently, one can describe protein dynamics as a superposition of two types of motions (9). The first type is the non-protein-specific motion, corresponding to harmonic vibrations of relatively small protein parts (e.g., amino-acid internal vibrations). The second is a large-amplitude protein-specific motion, which corresponds to the protein molecule transition from one CSS to another; these transitions are affected by the protein surroundings and are strongly hindered in a glassy matrix (10–23).

The CSSs are organized hierarchically, being grouped in tiers of different energy; their population controls the protein dynamics (4). Studies of the temperature dependence of the population of these CSSs were performed using infrared (IR) (24,25). Experimental data on the temperature dependence of the intensities of the Mössbauer and neutron scattering spectra (9,26–28) also were used to study the effect of the temperature and the solvent glass-liquid transition on the mean-square displacements of protein atoms. However, it was suggested recently (29) that the temperature dependence of these intensities stems mainly from the motion of the protein as a whole and do not reflect the internal protein dynamics.

The position of a band corresponding to the IR absorption by the heme-coordinated carbon monoxide is affected by the static protein electric field (30–40), whereas the temperature dependence of the shape of this band is sensitive to the dynamics of the heme environment (41–43). The CO band width of horseradish peroxidase (HRP(CO)) manifests very specific temperature-dependence: it weakly changes at temperatures lower than the temperature of the glass-liquid transition (T_c = 170–180 K) of the solvent (glycerol/water, pH 6.0 and pH 9.3) and increases dramatically upon heating in the liquid solvent. Earlier (41,42) we analyzed the temperature dependence of the second moment (M_2) of this band and showed that this broadening is caused by the transition of the protein between the CSSs of the lower- and higher-energy

Submitted June 8, 2005, and accepted for publication August 23, 2006.

Address reprint requests to S. S. Stavrov, Tel.: 972-3-640-9859; E-mail: stavrov@post.tau.ac.il.

0006-3495/06/12/4191/10 $2.00

doi: 10.1529/biophysj.105.068254

sets (CSS_l and CSS_h, respectively). However, in the procedure of the evaluation of the second moments the additional uncertainty originates, which, in particular, strongly depends on the correct subtraction of the background. Therefore, the precision of the obtained parameters did not allow us to make conclusions about the nature of this state.

In this article we use the theory of optical band shape (44–46) to interpret the experimental data on the temperature dependence of the shape (not only of M_2) of the CO band of HRP(CO) at pH 6.0 and 9.3 using simultaneous fitting procedures of the spectra obtained at different temperatures. This allows us to obtain the parameters of CSS_h and, as a result, suggest the nature of this state. Using this knowledge we also discuss the effect of the trehalose glass and substrate coordination on the dynamics and function of HRP, as well as the relationship between solvent-dependent and -independent protein motions and the resultant influence of the solvent on the heme center.

Theoretical background

Our previous theoretical studies of the effect of electric field on the CO vibrational frequency (Ω) showed that 1 Å motion of a unit point charge changes Ω by the order of 10 cm^{-1} (32,34). This implies that there must be weak coupling between the C–O stretching coordinate and motion of the charged or polar parts of the heme environment. This is pure dephasing, caused by this interaction, that mainly contributes to the thermal broadening of the CO band; the contribution of the relaxation processes hardly affects this dependence (47).

The CO vibrational frequency (Ω = 1900–2000 cm^{-1}) is much higher than the energy of thermal motion at room temperature (~200 cm^{-1}). Thus, its excited vibrational states are hardly populated even at room temperature and barely contribute to the formation of the corresponding IR absorption band. Therefore (41,42), the temperature dependence of the CO band can be described in the framework of the Condon approximation of general theory of optical absorption bandshapes (44–46,48). Assuming that the environmental motion is harmonic and describing the coupling using linear approximation, one can write down the Hamiltonian

$$H_0 = \frac{\mathbf{P}^2}{2M} + \frac{\mathbf{p}^2}{2m} + \frac{1}{2}(1 + 2\alpha q)M\Omega^2 Q^2 + \frac{1}{2}m\omega^2 q^2, \qquad (1)$$

where $\mathbf{P}$ and $\mathbf{p}$, M and m, Ω and ω, and Q and q are moments, reduced masses, initial frequencies, and displacements along the normal coordinate consisting mainly of the C–O distance and the protein effective mode, respectively. The value α is a constant of the linear coupling between the q- and Q-displacements, which describes the degree of the effect of the heme environment electric field on Ω.

It was shown (49,50) that the coupling under consideration shifts the equilibrium position of the adiabatic surface of the first excited CO vibrational state along the q coordinate in respect to the ground state by

$$q_0 = -\alpha\frac{\hbar\Omega}{m\omega^2}. \qquad (2)$$

It follows from general theory (44–46,48) that, in the case of rigid shift of the excited state in respect to the ground, the 0^{th} and first moments of the corresponding absorption band do not depend on temperature. The second moment (M_2) manifests very specific temperature dependence,

$$M_2(T) = A + \frac{1}{2}B\hbar\omega \times \coth\left(\frac{\hbar\omega}{2k_BT}\right), \qquad (3)$$

where

$$B = \frac{\alpha^2(\hbar\Omega)^2}{m\omega^2} \qquad (4)$$

characterizes both the strength of the coupling under consideration and elasticity constant of the heme environment motion $m\omega^2$; k_B is the Boltzmann constant; and $A \geq 0$ is a temperature-independent contribution of inhomogeneous broadening or zero temperature high-frequency vibrations, which hardly change their amplitudes in the temperature interval under investigation.

In the classical limit

$$\hbar\omega \ll k_BT, \qquad (5)$$

the band has a Gaussian shape, the second moment of which is

$$\sigma^2(T) = A + Bk_BT. \qquad (6)$$

Note that, in the case of strong inhomogeneous contribution (as is usually the case in protein systems because of their distribution over different CSSs of the same set), the bandshape is also close to Gaussian, for which the M_2 value depends on the temperature according to Eqs. 3 and 6.

The relationship

$$\frac{\partial(2kT/\hbar\omega)}{\partial T} > \frac{\partial\left[\coth\left(\frac{\hbar\omega}{2kT}\right)\right]}{\partial T} \qquad (7)$$

implies that, in the case of harmonic motion along the q-coordinate, M_2 cannot increase steeper than proportional to T.

RESULTS

We consider different simplest models of the heme environment dynamics, which can be used to interpret the experimental data. Two of them are based on an assumption that the heme environment explores only one low-energy set of CSSs, whereas other models take into account a possibility of thermal population also of higher-energy CSSs. Note that, below, the term ''heme environment'' will be used to

describe only a part of the whole heme environment that notably affects the CO bandshape.

Models of the heme environment dynamics

1. The energy of CSS_h is too high to be populated, and the heme environment motion is not affected by the glass-liquid transition. In this case the motion of the environment is harmonic and M_2 is expected to have the characteristic temperature-dependence of Eq. 3 or, if the classic limit (Eq. 5) is fulfilled, Eq. 6.
2. The CSS_h has too high an energy to be populated, but the heme environment motion is affected by the formation of the glassy matrix below the temperature of the glass-liquid transition (T_c); such formation freezes-down motions of the heme environment coupled to the CO IR transition. Taking into account that the glass-liquid transition is narrow (see, for example, (41,51)), its width can be neglected; therefore we assume that in the liquid sample ($T > T_c$) the motion of the environment is harmonic, whereas at $T < T_c$ it is frozen-out (4). In this case, if

$$\hbar\omega \ll k_B T_c, \tag{8}$$

the band has Gaussian shape with second moment

$$\sigma^2(T_{eff}) = A + Bk_B T_{eff}, \tag{9}$$

where

$$T_{eff} = \left\{ \begin{matrix} T, & T \geq T_c \\ T_{c,} & T < T_c \end{matrix} \right\}. \tag{10}$$

3. The protein including the heme environment can exist in CSS_l and CSS_h, whereas the transition between them is linked to the protein surface. However, in each of CSSs, the heme environment motion is disconnected from the protein surface and is harmonic in the whole interval of temperatures.

   In this case, the CSS_h population can be described using T_{eff} (Eq. 10) as

$$p(T_{eff}) = \left\{ 1 + \exp\left[\frac{\Delta F(T_{eff})}{k_B T_{eff}} \right] \right\}^{-1}, \tag{11}$$

   where ΔF is a difference in free energy between CSS_h and CSS_l,

$$\Delta F = \Delta E - \Delta S \cdot T_{eff}. \tag{12}$$

   Then, in the case of the harmonic motion in each CSS and strong inhomogeneous contribution, the CO band is described by the expression

$$F(\Omega) = I_0 \{ p(T_{eff})\, G[\Omega - \Omega_h, \sigma_h^2(T)] + [1 - p(T_{eff})]\, G[\Omega - \Omega_l, \sigma_l^2(T)] \}, \tag{13}$$

   where I_0 is the band intensity, $G[\Omega\text{–}\Omega_{h(l)}, \sigma^2_{h(l)}(T)]$ is a normalized Gaussian with maximum at $\Omega_{h(l)}$ and second moment of $\sigma^2_{h(l)}(T)$, which corresponds to the absorption by $CSS_{h(l)}$. The temperature dependence of $\sigma^2_{h(l)}(T)$ is described by Eq. 3, with constants $A_{h(l)}$ and $B_{h(l)}$.

   The temperature dependence of M_2 of the band can be easily obtained using Eq. 13:

$$M_2(F) = p(T_{eff})\sigma_h^2 + [1 - p(T_{eff})]\sigma_l^2 + p(T_{eff})[1 - p(T_{eff})](\Omega_h - \Omega_l)^2. \tag{14}$$

4. The glassy matrix arrests the motion of the heme environment in each of CSSs and does not affect the transition between them. The band has shape, described by Eq. 13, where T has to be substituted for T_{eff} and vice versa, $T \leftrightarrow T_{eff}$. Note that from the physical point of view this model does not look reasonable; the fitting procedure presented below supported this conclusion.
5. Both the transition between CSS_l and CSS_h and the motion in each of these CSSs are connected to the protein surface and, consequently, are frozen in the glassy matrix. In this case the bandshape depends on the temperature only in the liquid sample; this point can be described mathematically substituting $T \rightarrow T_{eff}$ in Eq. 13.
6. Neither the transition between CSS_l and CSS_h, nor the motions in each of the states are connected to the protein surface. In this case, the bandshape is described by Eq. 13 with $T_{eff} \rightarrow T$.

The HRP(CO) spectra

It was shown earlier (41,42) that heating of the liquid samples of HRP(CO) in the liquid 60% glycerol/water (v/v) solvent at pH 6.0 and 9.3 causes very strong increase of M_2 of the CO band, which is much steeper than proportional to T. In Eq. 7, this unambiguously shows that, in the liquid solution, the heme environment moves anharmonically. At the same time, thermal broadening of the CO band at $T < T_c$ could be well described in the framework of the harmonic model (Eq. 3).

Models 1 and 2 cannot explain such behavior of the band and should be ruled out. Models 3–6 differ only by their behavior at $T < T_c$ and include thermal population of CSS_h, which can lead to the experimentally observed broadening of the CO band.

To make the fitting procedure faster, only nine representative spectra, which correspond to the glassy (five spectra) and liquid (four spectra) samples ($T_c = 180$ K (41)) and span the whole experimental interval of temperatures, were considered. The fitting was performed using the Levenberg-Marquardt procedure. To accommodate the experimental uncertainty, the rigid shift of the band and up to 5% variation of the intensity (I_0) upon the temperature change was allowed. Taking into account the fact that all the spectra are relatively narrow, we simulated the background by a baseline.

The result of the fitting procedure showed that only Model 3 gives a reasonable fit. The fitting procedure automatically

led to the conclusion that $B_l = 0$ (see Eq. 4)—implying that CSS_l hardly contributes to the thermal broadening in both the samples. It was also obtained that criterion 5 is fulfilled in both the samples and the spectra were fitted in the classical limit (see Fig. 1 and Table 1 for the fitting parameters). Note, that the fitting procedure leads to slightly different Ω_h and Ω_l values for the spectra measured at different temperatures, the difference between them being constant. Their mean values are presented in Table 1, and the standard deviations of the Ω_l and Ω_h distributions in the pH 6.0 and 9.3 samples are 0.5 and 0.6 cm^{-1}, respectively. These deviations are in the range of the experimental uncertainty.

Note that postulating of the intensity independence of temperature and simultaneous fitting of all of the spectra allowed taking into account the contribution of broad and low-intense subbands (see, for example, spectra at 170 and 290 K in Fig. 2). If the fitting had been done for each temperature separately, these contributions would easily escape into erroneously determined background. This could lead to an incorrect conclusion about the reduction of the CO band intensity upon heating.

M_2 of A_0 band of Mb(CO)

M_2 of this band also increases very steeply upon heating in the liquid solvent (see Fig. 4 *a*) and cannot be interpreted in the framework of the harmonic approximation (24). It is successfully fitted to Eq. 14, neglecting the shift of the CO band upon the $CSS_l \rightarrow CSS_h$ transition ($\Omega_h = \Omega_l$) (fitting parameters are presented in Table 1). Note that, as remarked in the Introduction, the uncertainty of the obtained parameters is larger than in cases of fitting of spectra by themselves.

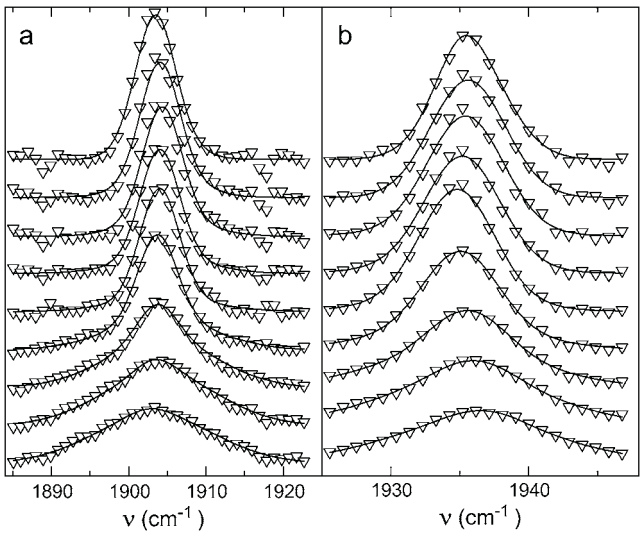

FIGURE 1 Temperature dependence of the CO infrared absorption band of HRP(CO) in glycerol/water solvent at pH 6.0 (*a*) and pH 9.3 (*b*) (41,42). The spectra from top to bottom correspond to the temperatures 12 (15 in the case of the pH 9.3 sample), 50, 90, 130, 170, 200, 230, 260, and 290 K. The solid curves represent the theoretical fit to the experimental data (*triangles*), obtained by using Model 3. In all spectra the background was subtracted.

M_2 of A_1 bands of Mb(CO) and Hb(CO), and of the CO band of HRP(CO) with aromatic substrate analog, benzohydroxamic acid (BHA)

Temperature dependences of M_2 of the A_1 band of Mb(CO) and Hb(CO), and of the CO infrared absorption band of HRP(CO)+BHA, are presented on Fig. 4 *b*. In this case, the M_2 increase upon heating is much weaker, than in the case of HRP(CO) and can be fitted to Model 2. The fitting parameters are presented in Table 1.

M_2 of the CO band of HRP(CO) in trehalose

The temperature dependence of M_2 of the central peak of the HRP(CO) spectrum in trehalose can be fitted in the framework of the harmonic approximation to Model 1, Eq. 3, the fitting parameters being $A = 1.4 \pm 0.4$ cm^{-2}, $B = 0.17 \pm 0.01$ cm^{-1}, and $\omega = 223 \pm 18$ cm^{-1}.

DISCUSSION

Modeling the heme environment dynamics in HRP(CO)

As it was noted in Results, Models 1 and 2 cannot explain the anharmonic temperature dependence of the infrared absorption CO band of HRP(CO) at pH 6.0 and 9.3.

Models 3–6 include the anharmonicity (thermal population of CSS_h) and in principle can cause the very strong thermal broadening. However, it is very difficult to imagine how the glassy matrix can arrest the motion inside each of CSSs and does not arrest the transition between CSSs, the latter being expected to cause much stronger change in the protein geometry. This explains why Model 4 fails to fit to the experimental data.

Model 5 assumes that the heme environment dynamics, and, consequently, the CO bandshape are temperature-independent in the glassy matrix. To understand why it does not work, one should carefully inspect the temperature dependence of the experimental spectra (see Fig. 2). It follows from Fig. 2 that the 12(15) K spectra notably differ from the corresponding 170 K spectra, the 170 K spectra having much longer tails. This shows that the heme environment motion depends on temperature even at $T < T_c = 180$ K.

Model 6, which assumes that the populations of CSS_h and CSS_l are changing even in the glassy matrix, leads to the too-strong temperature dependence of the bandshape at $T < T_c$.

Model 3 fits well to the experimental data. Fig. 2 clearly shows how the increasing amplitude of heme environment motion in CSS_h upon heating leads to the appearance of the band tails in the glassy matrix. It is also clearly seen how the

TABLE 1 Spectroscopic and dynamic parameters of the studied proteins

	ΔE cm^{-1}	ΔS e.u.	A_h cm^{-2}	B_h cm^{-1}	A_l cm^{-2}	B_l cm^{-1}	Ω_h cm^{-1}	Ω_l cm^{-1}
HRP(CO) pH 9.3 (model 3)	1325 ± 120	6.2 ± 0.6	0	0.22 ± 0.02	6.9 ± 0.14	0	1935.6 ± 0.6	1934.8 ± 0.6
HRP(CO) pH 6.0 (model 3)	1453 ± 145	7.2 ± 0.6	12.0 ± 4.2	0.24 ± 0.04	6.0 ± 0.2	0	1904.3 ± 0.5	1903.7 ± 0.5
A_0 band, Mb(CO) pH 5.0 (model 3)	1805 ± 315	7.8 ± 0.8	37.2 ± 8.3	0.04 ± 0.05	15.8 ± 1.2	0	1966.0	1966.0
HRP(CO)+BHA pH 6.0 (model 2)	—	—	—	—	0	0.07 ± 0.05	—	—
A_1 band, Mb(CO) pH 6.8 (model 2)	—	—	—	—	0	0.12 ± 0.03	—	—
A_1 band, Hb(CO) pH 6.8 (model 2)	—	—	—	—	7.35	0.04 ± 0.005	—	—

heating in the liquid solvent increases population of CSS_h, causing essentially non-Gaussian bandshape at 230 K, where CSS_l and CSS_h are nearly equally populated. Further heating strongly reduces the contribution of CSS_l into the spectrum, signaling an almost complete transition of the system in CSS_h.

The temperature dependence of the CSS_h population can be calculated using Eq. 11 and the corresponding parameters of Table 1. Fig. 3 shows that the population strongly depends on the temperature, and at 290 K ~95% of the protein molecules in the pH 6.0 sample exist in CSS_h, and ~90% in the pH 9.3 sample. It follows from Fig. 3 that, in the samples with a solvent with $T_c < 180$ K, the band is expected to manifest stronger temperature dependence at $T < 180$ K than in the glycerol/water sample. This conclusion can be tested experimentally.

Note that, in principle, Models 3–6 could be generalized by invoking a larger number of the higher-energy sets of the CSSs. However, this generalization would increase a number of parameters. Since the temperature dependence under consideration is described in the framework of Model 3, this generalization would be superfluous.

Nature of the excited conformational substate

The simplest explanation for the nature of CSS_h would be to suggest that it corresponds to a different protein conformation, in which the amino acids forming the HRP heme pocket move with much larger amplitude than in CSS_l. The cause of this larger dynamics could be a cleavage of some hydrogen bonds that exist in CSS_l and anchor some specific amino acid. However, the close inspection of the magnitudes of parameters presented in Table 1 shows that this suggestion is most probably wrong.

The pK_α of the HRP(CO) distal histidine (His^{42}) was reported to be 8.3 (52–55). Increasing pH above this value causes the deprotonation of His^{42}, transforming its positively charged imidazolinium to neutral imidazole, which has a moderate dipole moment. This change alters the structure of the distal part of the heme pocket (43). The changes in the pocket structure and the His^{42} charge essentially affect the electrostatic interaction between the C–O dipole moment and the heme pocket amino acids. As a result, the CO band (40,43) notably shifts upon the change in pH from 6.0 to 9.3 (see Fig. 1).

Consequently, if the thermal broadening of the CO band was caused by the motion of the heme pocket amino acids, then the parameter of the electrostatic interaction of this motion with the C-O dipole moment (B in Eq. 4) would be essentially different at pH 6.0 and 9.3. However, it follows from Table 1 that B_h is weakly affected by the pH change, decreasing only by <10% upon the His^{42} deprotonation (this decrease is of the order of the uncertainty of the fitting procedure; see Table 1), whereas B_l is the same at both pH values. Moreover, the CO band position hardly shifts upon the transition of the protein from CSS_l to CSS_h in both the pH 6.0 and 9.3 samples; this fact points to the weak change in the heme pocket structure upon the transition. Therefore, one should conclude that, most probably, the CO band broadening is caused not by the increase in the heme pocket dynamics in CSS_h, but by some other factor.

From our point of view, the best candidate for this role is a disordered water molecule, which appears in the heme pocket upon heating, and CSS_l and CSS_h correspond to the protein conformation without and with this molecule in the heme pocket. Indeed, HRP has a big pocket, which can accommodate not only water, but also much bigger substrate molecules and their analogs (56,57), and the analysis of the crystal structure of ferric HRP suggests the presence of a disordered water molecule in the heme pocket (56). The pocket is less polar than the solvent, and therefore CSS_l corresponds to the protein conformation with the water molecule outside of the pocket. H_2O has a strong dipole moment; it can weakly bind in different places of the heme pocket and move at these places and between them, affecting the CO band width without notably changing its position. H_2O entry to the pocket from the solvent increases the entropy of the entire system; this qualitative conclusion coincides with the results of the fitting procedure (see Table 1). Moreover, at pH 6.0 (His^{42} is protonated) the heme pocket is more polar and has more places to bind H_2O, than at pH 9.3. Therefore, both the increase in entropy upon the water entrance (ΔS) and the

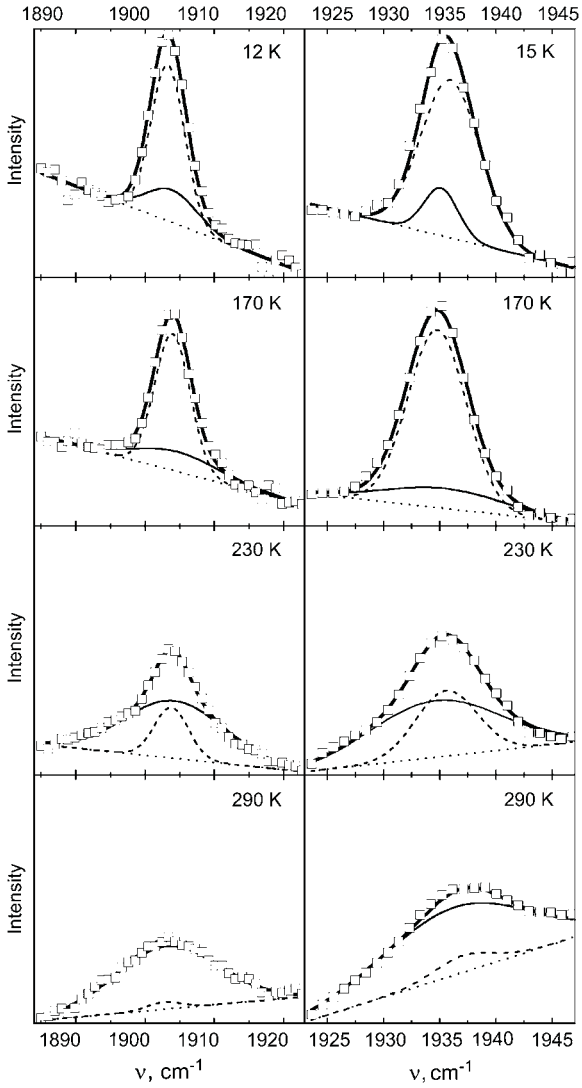

FIGURE 2 Temperature dependence of the contribution of CSS_l and CSS_h into the CO band (*thick solid curve* corresponds to the fit of the band; *dashed* and *thin solid curves* describe the contributions of CSS_l and CSS_h into the band, respectively; and the *dotted line* is background). The left and right columns correspond to the pH 6.0 and 9.3 samples, respectively.

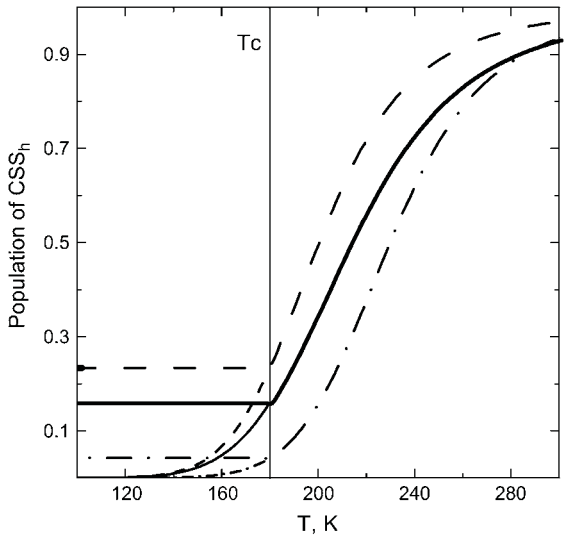

FIGURE 3 Temperature dependence of the population of the excited conformational substate in the HRP(CO) at pH 6.0 and 9.3 (*thick dashed* and *solid curves*, respectively) and of the open conformation of Mb(CO) at pH 5.0 (*thick dash-dotted curve*). The thin curves represent the would-be populations of CSS_h, if the samples were liquid in the whole interval of the temperatures.

inhomogeneous broadening in CSS_h (A_h) are expected to be stronger at pH 6.0 than at pH 9.3. This qualitative conclusion also coincides with the results of the fitting procedure (see Table 1; note, however, the uncertainty of the ΔS evaluation). Water motion inside the heme pocket is hardly connected to the protein surface and is expected to take place in CSS_h even in the glassy environment. On contrary, the water entrance into the pocket ($CSS_l \rightarrow CSS_h$ transition) is coupled to the large amplitude motions of the heme pocket, their arrest by the glassy matrix making water entrance impossible. The latter two features explain the ability of Model 3 (and only of Model 3) to fit the experimental data.

The appearance of the disordered water molecule in the heme pocket can be also caused by a cleavage upon heating of the hydrogen bond between one of the ordered heme pocket water molecules and the corresponding amino acid (56). We cannot exclude this possibility, but note that the presence of a hydrogen-bonded ordered water molecule in the pocket produces a static electric field. This field is expected to notably shift the CO band position. At the same time the disordered water molecule only broadens the band. Consequently, one should expect not only broadening, but also a notable shift of the CO band upon heating when the hydrogen bonded is cleaved and the water moves in the pocket. This conclusion is in contradiction to the very close values of Ω_l and Ω_h, and makes this mechanism less likely.

Additional x-ray diffraction experiments at low temperatures can be suggested to distinguish between these two mechanisms. If a water molecule enters the heme pocket at higher temperatures (in liquid solvent), the number of ordered water molecules at low and room temperatures is expected to be the same. On the contrary, if heating of the sample liberates an ordered hydrogen-bonded water molecule, the experiment must clearly show this.

It follows from the consideration presented above that position of the CO band in HRP(CO) is controlled by the electrostatic interaction with heme pocket amino acids (43), whereas main contribution to the band broadening most probably stems from the interaction with the disordered water molecule in the pocket.

Other heme proteins

On Fig. 4 *a*, the temperature dependences of M_2 of the CO bands of HRP(CO) at pH 6.0 and 9.3 (calculated using Eq. 14 and parameters from Table 1) and of the A_0 band of Mb(CO)

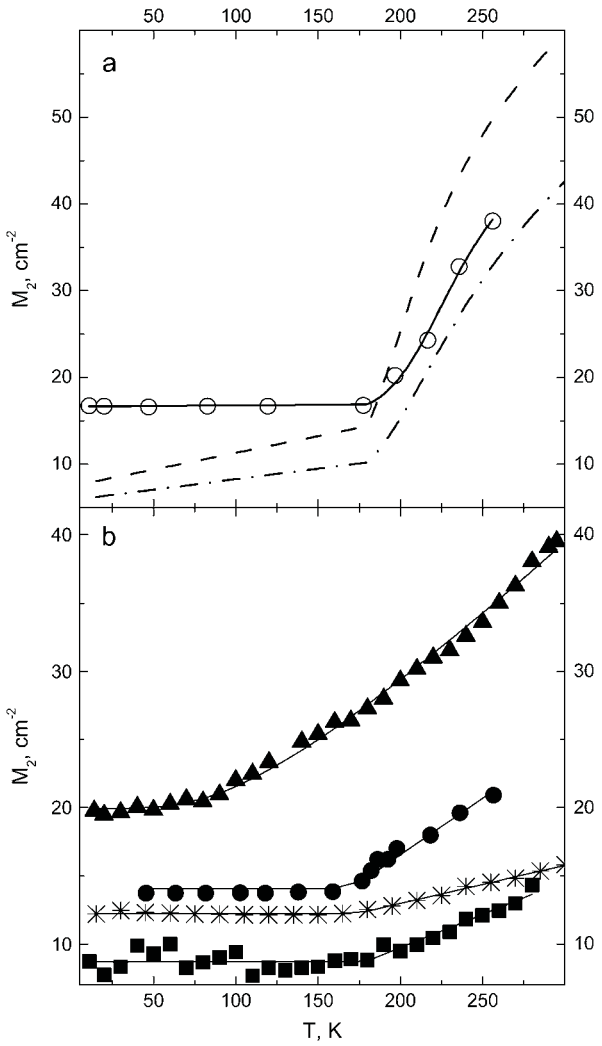

FIGURE 4 Temperature dependence of M_2 of the CO IR absorption band of different proteins. (*a*) HRP(CO) at pH 6.0 (*dashed curve*) and 9.3 (*dashed-dotted curve*), and A_0 component of the open conformation of Mb(CO) at pH 5.0 (*open circles*) (24); (*b*) central component of HRP(CO) in trehalose glass at pH 6.0 (*solid triangles*) (42); A_1 component of the closed conformation of Mb(CO) at pH 6.8 (*solid circles*) (24); A_1 component of the closed conformation of Hb(CO) at pH 7.0 (*asterisks*) (67); and HRP(CO)+BHA at pH 6.0 (*solid squares*) (41). Solid curves represent fits to different models as described in the text.

at pH 5.0 (24) are presented. The A_0 CO infrared absorption band was shown (34,58–61) to correspond to the open protein conformation with the distal histidine located outside of the heme pocket. In this conformation the distal part of the heme pocket is big enough to accommodate nitrite (62) as well as the water molecule. The myoglobin heme pocket is hydrophobic; consequently the CSS_l must correspond to the state with the water molecule out of the pocket. Upon heating, the water molecule can enter the pocket, forming CSS_h. This naturally explains why Model 3, which involves an assumption about the presence of CSS_h, fits in the experimental data. Our interpretation of CSS_h as CSS with a disordered water in the pocket is also supported by the fact that the band position hardly depends on the temperature (24), suggesting a small difference between Ω_h and Ω_l. Note that this result reinstates an earlier proposition (25,63) that, in the open conformation, there is CSS_h (called A'_0 by the authors). Population of this CSS_h strongly increases upon heating (see Fig. 3), being lower than for HRP in nearly the entire interval of the temperatures studied. This result is easily understandable, because the Mb heme pocket is much smaller and less polar than that of HRP.

In the closed conformation, which is mostly populated at pH 6.8, the distal histidine is located inside the heme pocket, leaving much less free space. Consequently, the CSS_h energy is much higher and its population is expected to be much less. As a result, it hardly contributes to the CO band, and the thermal broadening temperature dependence of the related A_1 CO band is expected to behave harmonically in the liquid solvent. In the glassy environment, the band is expected to depend on temperature harmonically if the heme environment is not linked to the protein surface, and be temperature independent if the heme environment is strongly linked to the protein surface. Fitting shows (see Fig. 4 *b*) that, in the closed conformation of Mb(CO), the latter situation takes place (Model 2). The same is true for HRP(CO)+BHA and the closed conformation of Hb(CO), showing that the BHA binding in the HRP heme pocket displaces the disordered water even at room temperature (57). Most probably in all these cases the CO broadening is caused by the electrostatic coupling to the motions of the heme pocket amino acids, which are linked to the protein surface. This cause of the broadening also presumably exists in the CSS_h of the HRP(CO) and Mb(CO) open conformation, but is masked by a much stronger contribution of the disordered water.

It was obtained recently (64) that the distal histidine relaxation after the Mb(CO) photolysis is mostly disengaged from the solvent. However, as the authors (64) note, this disengagement most probably arises from the inward direction of the histidine relaxation movement. Moreover, this displacement is relatively small. On the contrary, in the open protein conformation the distal histidine is displaced significantly outward of the pocket; this displacement is expected to be strongly linked to solvent.

Trehalose ($T_c = 331$ K) exists in a glassy state in the entire interval of temperatures studied in this article. The infrared absorption spectra of the pH 6.0 sample of HRP(CO) in trehalose consist of three clearly distinct peaks, at least at low temperatures (42). This is very different from other HRP(CO) spectra (Fig. 1), which manifest only one absorption peak in the interval 1900–2000 cm^{-1}. In Fig. 4 *b*, the temperature dependence of M_2 of the most intense central peak is presented; despite the glassy environment, it significantly depends on temperature. This dependence was fitted to the harmonic model 1, Eq. 3, which suggests that there is no $CSS_l \rightarrow CSS_h$ transition. This dependence is much stronger than that of the closed conformations of Mb(CO),

Hb(CO), and HRP(CO)+BHA, where there is also no $CSS_l \rightarrow CSS_h$ transition. Moreover, this is the only case where the quantum effects are clearly seen and the effective frequency of the active vibration is found out: $\omega = 223\ cm^{-1}$. All these facts imply that, in this case, the heme pocket structure significantly differs from that in the glycerol/water mixture.

Three hypotheses can be invoked to explain the experimentally observed temperature dependence under consideration. First, the HRP(CO) trehalose sample contains disordered water. This is possible because the solid sample was prepared from the trehalose-water solution (42), and the probability for a water molecule to enter the pocket at $T > 300$ K in liquid solvent is close to 1 (see Fig. 3). Formation of the glassy matrix upon the sample drying can lock the water in the pocket keeping the system in CSS_h at all the temperatures studied. This assumption is supported by the close magnitudes of the coupling of the CO band to the heme environment: $B_h = 0.24 \pm 0.04$ (glycerol-water solvent) and 0.17 ± 0.01 (trehalose glass) cm^{-1}. The quantum effects in the temperature dependence can stem from the change in the water molecule motion, because in the glass under osmotic stress the protein in general and the heme environment in particular can become more compact.

Another possibility is that the reduction of the distances between the CO and the pocket amino acids upon the heme pocket contraction in the glassy matrix increases the coupling of the CO band to the internal vibrations of these amino acids. If this interpretation is correct, the 223 cm^{-1} is an effective frequency, which corresponds to a group of internal vibrations of the heme pocket amino acids.

And finally, the central peak of HRP(CO) in trehalose at pH 6.0 can correspond to the conformation with a trehalose molecule located in the pocket (despite its big size, trehalose is flexible and can enter the pocket). In this case, the stronger thermal broadening than in the cases of HRP(CO)+BHA, and closed conformations of Mb(CO) and Hb(CO) and the quantum effects, can be interpreted as a manifestation of the coupling of the CO band to internal vibration of the trehalose molecule. This assumption is supported by the facts that trehalose has vibrations in this region of 223 cm^{-1} (65) and another peroxidase accommodates a molecule of co-solvent, glycerol, in its pocket (66).

Note that in this article we constrained ourselves to the simplest model of the protein dynamics, which invokes only one CSS_h. It is clear that it can be (and probably are) several higher energy conformational states. However, the fact that the simplest model allows interpreting the experimental data successfully shows that no conclusions about the larger number of CSS_h and their nature can be done on the basis of the experimental data under consideration.

CONCLUSION

The temperature dependences of the infrared absorption CO bands of HRP(CO) at different pH values and of second moments of the CO bands of Mb(CO) and Hb(CO) were interpreted using the theory of optical absorption bandshape. The interpretation revealed very different dynamics of the heme environment in these proteins: anharmonic, caused by the presence of the high-energy CSS_h; harmonic in the liquid solvent and frozen-in by the glassy matrix; and harmonic in the whole interval of temperatures studied.

In HRP(CO) and the open conformation of Mb(CO) a high-energy set of CSS_h exists. Its population strongly increases upon heating and becomes close to 1 at room temperature. Most probably this CSS_h corresponds to the protein substate with a disordered water molecule in the heme pocket. It is clear that the disordered water is also expected to affect the structure and dynamics of the heme pocket itself. Note that, to our best knowledge, this is the first example of an almost complete transition of a native protein from a low-energy set of conformational substates to a high-energy one, caused by heating. It is the population of this CSS_h, which was shown to cause the anharmonic behavior of the CO bands under discussion.

In the HRP(CO)+BHA and closed conformations of Mb(CO) and Hb(CO) the disordered water is forced out of the pocket by BHA or the distal histidine. This strongly increases the CSS_h energy and causes a very small population of CSS_h, even at the highest studied temperatures. Thus, the only contribution to the thermal broadening of the CO band stems from the electrostatic coupling of the CO vibration to the amino acids of the heme pocket. Their motions are linked to the motion of the protein surface. Therefore these motions are frozen in the glassy matrix, whereas in the liquid solvent they are well described in the harmonic approximation. As the result, the CO band second-moment is temperature independent in the glassy matrix and is proportional to the temperature in a liquid solvent.

Finally, the harmonic behavior of the central CO peak in the infrared absorption spectra of HRP(CO) in trehalose manifests electrostatic coupling of the CO vibration to an oscillator which is disengaged from the protein surface motion.

Usually enzymes have big pockets near their active site, which can accommodate the substrates. These pockets are more hydrophobic than the protein environment. Therefore the water entrance in this pocket upon heating and its presence at room temperature can be a general property of different enzymes. It is obvious that change in the number of the disordered water molecules in the pocket should affect the mechanism and dynamics of the enzyme functioning and must be taken into account when interpreting the experimental data. For example, the enthalpy and entropy of the enzymatic reactions is usually obtained from the temperature dependence of their equilibrium and rate constants. Doing so, one must remember that most probably the temperature change affects the population of different sets of the enzyme's conformational substates, which differ by the number of disordered water molecules in the active site pocket.

We thank Dr. A. Cupane for providing us with the Hb(CO) experimental data and Dr. N. Agmon for very useful discussions.

This work was supported by National Institutes of Health grant No. GM 48130.

REFERENCES

1. Rousseau, D. L., and J. M. Friedman. 1988. Transient and cryogenic studies of photodissociated hemoglobin and myoglobin. *In* Biological Application of Raman Spectroscopy. T. G. Spiro, editor. Wiley & Sons, New York. 133–215.
2. Parak, F. G., and G. U. Nienhaus. 2002. Myoglobin, a paradigm in the study of protein dynamics. *ChemPhysChem.* 3:249–254.
3. Austin, R. H., K. W. Beeson, L. Eisenstein, H. Frauenfelder, and I. C. Gunsalus. 1975. Dynamics of ligand binding to myoglobin. *Biochemistry.* 14:5355–5373.
4. Frauenfelder, H., P. G. Wolynes, and R. H. Austin. 1999. Biological physics. *Rev. Mod. Phys.* 71:S419–S430.
5. Angiolillo, P. J., J. S. J. Leigh, and J. M. Vanderkooi. 1982. Resolved fluorescence emission spectra of iron-free cytochrome c. *Photochem. Photobiol.* 36:133–137.
6. Kaposi, A. D., W. W. Wright, and J. M. Vanderkooi. 2003. Consequences of inhomogeneous broadening on fluorescence line narrowing spectra. *J. Fluoresc.* 13:59.
7. Fidy, J., M. Laberge, A. D. Kaposi, and J. M. Vanderkooi. 1998. Fluorescence line narrowing applied to the study of proteins. *Biochim. Biophys. Acta Protein Struct. Mol. Enzymol.* 1386:331–351.
8. Kaposi, A. D., and J. M. Vanderkooi. 1992. Vibronic energy map and excited-state vibrational characteristics of magnesium myoglobin determined by energy-selective fluorescence. *Proc. Natl. Acad. Sci. USA.* 89:11371–11375.
9. Parak, F., and E. W. Knapp. 1984. A consistent picture of protein dynamics. *Proc. Natl. Acad. Sci. USA.* 81:7088–7092.
10. Cupane, A., M. Leone, E. Vitrano, and L. Cordone. 1988. Structural and dynamic properties of the heme pocket in myoglobin probed by optical spectroscopy. *Biopolymers.* 27:1977–1997.
11. Cordone, L., A. Cupane, M. Leone, and E. Vitrano. 1986. Optical absorption spectra of deoxy- and oxyhemoglobin in the temperature range 300–20 K. Relation with protein dynamics. *Biophys. Chem.* 24: 259–275.
12. Frauenfelder, H., N. A. Alberding, A. Ansari, D. Braunstein, B. R. Cowen, M. K. Hong, I. E. T. Iben, J. B. Johnson, S. Luck, M. C. Marden, J. R. Mourant, P. Ormos, L. Reinisch, R. Scholl, A. Schulte, E. Shyamsunder, L. B. Sorensen, P. J. Steinbach, A. H. Xie, R. D. Young, and K. T. Yue. 1990. Proteins and pressure. *J. Phys. Chem.* 94:1024–1037.
13. Hagen, S. J., J. Hofrichter, and W. A. Eaton. 1996. Geminate rebinding and conformational dynamics of myoglobin embedded in a glass at room temperature. *J. Phys. Chem.* 100:12008–12021.
14. Gottfried, D. S., E. S. Peterson, A. G. Sheikh, J. Q. Wang, M. Yang, and J. M. Friedman. 1996. Evidence for damped hemoglobin dynamics in a room temperature trehalose glass. *J. Phys. Chem.* 100:12034–12042.
15. Cottone, G., L. Cordone, and G. Ciccotti. 2001. Molecular dynamics simulation of carboxy-myoglobin embedded in a trehalose-water matrix. *Biophys. J.* 80:931–938.
16. Cordone, L., M. Ferrand, E. Vitrano, and G. Zaccai. 1999. Harmonic behavior of trehalose-coated carbon-monoxy-myoglobin at high temperature. *Biophys. J.* 76:1043–1047.
17. Hagen, S. J., J. Hofrichter, and W. A. Eaton. 1995. Protein reaction-kinetics in a room-temperature glass. *Science.* 269:959–962.
18. Huang, J., A. Ridsdale, J. Q. Wang, and J. M. Friedman. 1997. Kinetic hole burning, hole filling, and conformational relaxation in heme proteins: direct evidence for the functional significance of a hierarchy of dynamical processes. *Biochemistry.* 36:14353–14365.
19. Schlichter, J., and J. Friedrich. 2001. Glasses and proteins: similarities and differences in their spectral diffusion dynamics. *J. Chem. Phys.* 114:8718–8721.
20. Gafert, J., J. Friedrich, and F. Parak. 1993. A comparative pressure tuning hole-burning study of protoporphyrin-IX in myoglobin and in a glassy host. *J. Chem. Phys.* 99:2478–2486.
21. Stavrov, S. S. 2001. Optical absorption band III of deoxyheme proteins as a probe of their structure and dynamics. *Chem. Phys.* 271:145–154.
22. Stavrov, S. S. 2004. Correct interpretation of heme protein spectra allows distinguishing between the heme and the protein dynamics. *Biopolymers.* 74:37–40.
23. Prabhu, N. V., S. D. Dalosto, K. A. Sharp, W. W. Wright, and J. M. Vanderkooi. 2002. Optical spectra of Fe^{II} cytochrome c interpreted using molecular dynamics simulations and quantum mechanical calculations. *J. Phys. Chem. B.* 106:5561–5571.
24. Ansari, A., J. Berendzen, D. Braunstein, B. R. Cowen, H. Frauenfelder, M. K. Hong, I. E. T. Iben, J. B. Johnson, P. Ormos, T. B. Sauke, R. Scholl, A. Schulte, P. J. Steinbach, J. Vittitow, and R. D. Young. 1987. Rebinding and relaxation in the myoglobin pocket. *Biophys. Chem.* 26:337–355.
25. Hong, M. K., D. Braunstein, B. R. Cowen, H. Frauenfelder, I. E. T. Iben, J. R. Mourant, P. Ormos, R. Scholl, A. Schulte, P. J. Steinbach, A. H. Xie, and R. D. Young. 1990. Conformational substates and motions in myoglobin—external influences on structure and dynamics. *Biophys. J.* 58:429–436.
26. Bicout, D. J., and G. Zaccai. 2001. Protein flexibility from the dynamical transition: a force constant analysis. *Biophys. J.* 80:1115–1123.
27. Zaccai, G. 2003. Proteins as nano-machines: dynamics-function relations studied by neutron scattering. *J. Phys. Cond. Matter.* 15: S1673–S1682.
28. Doster, W., S. Cusack, and W. Petry. 1989. Dynamical transition of myoglobin revealed by inelastic neutron-scattering. *Nature.* 337:754–756.
29. Chong, S. H., Y. Joti, A. Kidera, N. Go, A. Ostermann, A. Gassmann, and F. Parak. 2001. Dynamical transition of myoglobin in a crystal: comparative studies of x-ray crystallography and Mossbauer spectroscopy. *Eur. Biophys. J. Biophys. Lett.* 30:319–329.
30. Park, K. D., K. Guo, F. Adebodun, M. L. Chiu, S. G. Sligar, and E. Oldfield. 1991. Distal and proximal ligand interactions in heme proteins: correlations between C-O and Fe-C vibrational frequencies, oxygen-17 and carbon-13 nuclear magnetic resonance. *Biochemistry.* 30:2333–2347.
31. Ray, G. B., X. Y. Li, J. A. Ibers, J. L. Sessler, and T. G. Spiro. 1994. How far can proteins bend the FeCO unit? Distal polar and steric effects in heme-proteins and models. *J. Am. Chem. Soc.* 116:162–176.
32. Kushkuley, B., and S. S. Stavrov. 1996. Theoretical study of the distal-side steric and electrostatic effects on the vibrational characteristics of the FeCO unit of the carbonylheme proteins and their models. *Biophys. J.* 70:1214–1229.
33. Kushkuley, B., and S. S. Stavrov. 1997. Theoretical study of the electrostatic and steric effects on the spectroscopic characteristics if the metal-ligand unit of heme proteins. 3. Vibrational properties of Fe(III)CN. *Biochim. Biophys. Acta Protein Struct. Mol. Enzymol.* 1341:238–250.
34. Kushkuley, B., and S. S. Stavrov. 1997. Theoretical study of the electrostatic and steric effects on the spectroscopic characteristics of the metal-ligand unit of heme proteins. 2. C-O vibrational frequencies, O-17 isotropic chemical shifts, and nuclear quadrupole coupling constants. *Biophys. J.* 72:899–912.
35. Phillips, J. G. N., M. L. Teodoro, T. Li, B. Smith, and J. S. Olson. 1999. Bound CO is a molecular probe of electrostatic potential in the distal pocket of myoglobin. *J. Phys. Chem. B.* 103:8817–8829.
36. Manas, E. S., J. M. Vanderkooi, and K. A. Sharp. 1999. The effects of protein environment on the low temperature electronic spectroscopy of cytochrome c and microperoxidase-11. *J. Phys. Chem. B.* 103:6334–6348.

37. Franzen, S. 2002. An electrostatic model for the frequency shifts in the carbonmonoxy stretching band of myoglobin: correlation of hydrogen bonding and the Stark tuning rate. *J. Am. Chem. Soc.* 124:13271–13281.

38. Dalosto, S. D., J. M. Vanderkooi, and K. A. Sharp. 2004. Vibrational stark effects on carbonyl, nitrile, and nitrosyl compounds including heme ligands, CO, CN, and NO, studied with density functional theory. *J. Phys. Chem. B.* 108:6450–6457.

39. Dalosto, S. D., N. V. Prabhu, J. M. Vanderkooi, and K. A. Sharp. 2003. A density functional theory study of conformers in the ferrous CO complex of horseradish peroxidase with distinct Fe-C-O configurations. *J. Phys. Chem. B.* 107:1884–1892.

40. Kaposi, A. D., W. W. Wright, J. Fidy, S. S. Stavrov, J. M. Vanderkooi, and I. Rasnik. 2001. Carbonmonoxy horseradish peroxidase as a function of pH and substrate: influence of local electric fields on the optical and infrared spectra. *Biochemistry.* 40:3483–3491.

41. Kaposi, A. D., J. M. Vanderkooi, W. W. Wright, J. Fidy, and S. S. Stavrov. 2001. Influence of static and dynamic disorder on the visible and infrared absorption spectra of carbonmonoxy horseradish peroxidase. *Biophys. J.* 81:3472–3482.

42. Stavrov, S. S., W. W. Wright, J. M. Vanderkooi, J. Fidy, and A. D. Kaposi. 2002. Optical and IR absorption as probe of dynamics of heme proteins. *Biopolymers.* 67:255–258.

43. Kaposi, A. D., N. V. Prabhu, S. D. Dalosto, K. A. Sharp, W. W. Wright, S. S. Stavrov, and J. M. Vanderkooi. 2003. Solvent dependent and independent motions of CO-horseradish peroxidase examined by infrared spectroscopy and molecular dynamics calculations. *Biophys. Chem.* 106:1–14.

44. Rebane, K. K. 1970. Impurity spectra of solids. *In* Elementary Theory of Vibrational Structure. Plenum Press, New York.

45. Perlin, Y. E. 1964. Modern methods in the theory of many-phonon processes. *Uspekhi Fizicheskix Nauk.* 80:553–595.

46. Lax, M. 1952. The Franck-Condon principle and its application to crystals. *J. Chem. Phys.* 20:1752–1760.

47. Fayer, M. D. 2001. Fast protein dynamics probed with infrared vibrational echo experiments. *Annu. Rev. Phys. Chem.* 52:315–356.

48. Markham, J. J. 1959. Interaction of normal modes with electron traps. *Rev. Mod. Phys.* 31:956–989.

49. Bitler, A., and S. S. Stavrov. 1999. Iron-histidine resonance Raman band of deoxyheme proteins: effects of anharmonic coupling and glass-liquid phase transition. *Biophys. J.* 77:2764–2776.

50. Rosenfeld, Y. B., and S. S. Stavrov. 1994. Anharmonic coupling of soft modes and its influence on the shape of the iron-histidine resonance Raman band of heme-proteins. *Chem. Phys. Lett.* 229:457–464.

51. Demmel, F., W. Doster, W. Petry, and A. Schulte. 1997. Vibrational frequency shifts as a probe of hydrogen bonds: thermal expansion and glass transition of myoglobin in mixed solvents. *Eur. Biophys. J. Biophys. Lett.* 26:327–335.

52. Evangelista-Kirkup, R., G. Smulevich, and T. G. Spiro. 1986. Alternative carbon monoxide binding modes for horseradish peroxidase studied by resonance Raman spectroscopy. *Biochemistry.* 25:4420–4425.

53. Smulevich, G., M. Paoli, G. DeSanctis, A. R. Mantini, F. Ascoli, and M. Coletta. 1997. Spectroscopic evidence for a conformational transition in horseradish peroxidase at very low pH. *Biochemistry.* 36: 640–649.

54. Feis, A., J. N. Rodriguez-Lopez, R. N. F. Thorneley, and G. Smulevich. 1998. The distal cavity structure of carbonyl horseradish peroxidase as probed by the resonance Raman spectra of His-42-Leu and Arg-38-Leu mutants. *Biochemistry.* 37:13575–13581.

55. Uno, T., Y. Nishimura, M. Tsuboi, R. Makino, T. Iizuka, and Y. Ishimura. 1987. Two types of conformers with distinct Fe-C-O configuration in the ferrous CO complex of horseradish peroxidase. Resonance Raman and infrared spectroscopic studies with native and deuteroheme-substituted enzymes. *Biochemistry.* 262:4549–4556.

56. Gajhede, M., D. J. Schuller, A. Henriksen, A. T. Smith, and T. L. Poulos. 1997. Crystal structure of horseradish peroxidase C at 2.15 Ångstrom resolution. *Nat. Struct. Biol.* 4:1032–1038.

57. Henriksen, A., D. J. Schuller, K. Meno, K. G. Welinder, A. T. Smith, and M. Gajhede. 1998. Structural interactions between horseradish peroxidase C and the substrate benzohydroxamic acid determined by x-ray crystallography. *Biochemistry.* 37:8054–8060.

58. Morikis, D., P. M. Champion, B. A. Springer, and S. G. Sligar. 1989. Resonance Raman investigations of site-directed mutants of myoglobin: effects of distal histidine replacement. *Biochemistry.* 28:4791–4800.

59. Zhu, L., J. T. Sage, A. A. Rigos, D. Morikis, and P. M. Champion. 1992. Conformational Interconversion in protein crystals. *J. Mol. Biol.* 224:207–215.

60. Yang, F., and J. G. N. Phillips. 1996. Crystal structure of CO^{-}, deoxy- and met-myoglobins at various pH values. *J. Mol. Biol.* 256:762–774.

61. Muller, J. D., B. H. McMahon, E. Y. T. Chien, S. G. Sligar, and G. U. Nienhaus. 1999. Connection between the taxonomic substates and protonation of histidines 64 and 97 in carbonmonoxy myoglobin. *Biophys. J.* 77:1036–1051.

62. Frauenfelder, H., B. H. McMahon, R. H. Austin, K. Chu, and J. T. Groves. 2001. The role of structure, energy landscape, dynamics, and allostery in the enzymatic function of myoglobin. *Proc. Natl. Acad. Sci. USA.* 98:2370–2374.

63. Iben, I. E. T. 1988. The kinetics of protein conformational relaxation in sperm whale myoglobin following a pressure jump. PhD thesis, University of Illinois at Urbana-Champaign.

64. Dantsker, D., U. Samuni, J. M. Friedman, and N. Agmon. 2005. A hierarchy of functionally important relaxations within myoglobin based on solvent effects, mutations and kinetic model. *BBA Proteins Proteomics.* 1749:234–251.

65. Ballone, P., M. Marchi, C. Branca, and S. Magazu. 2000. Structural and vibrational properties of trehalose: a density functional study. *J. Phys. Chem. B.* 104:6313–6317.

66. Gupta, K., B. S. Selinsky, C. J. Kaub, A. K. Katz, and P. J. Loll. 2004. The 2.0 Å resolution crystal structure of prostaglandin H-2 synthase-1: structural insights into an unusual peroxidase. *J. Mol. Biol.* 335: 503–518.

67. Cupane, A., M. Leone, and V. Militello. 2003. Conformational substates and dynamic properties of carbonmonoxy hemoglobin. *Biophys. Chem.* 104:335–344.